Control of a Non-Orthogonal Reconfigurable Machine Tool

Reuven Katz

John Yook

Yoram Koren

Computerized control systems for machine tools must generate coordinated movements of the separately driven axes of motion in order to trace accurately a predetermined path of the cutting tool relative to the workpiece. However, since the dynamic properties of the individual machine axes are not exactly equal, undesired contour errors are generated. The contour error is defined as the distance between the predetermined and actual path of the cutting tool. The cross-coupling controller (CCC) strategy was introduced to effectively decrease the contour errors in conventional, orthogonal machine tools. This paper, however, deals with a new class of machines that have non-orthogonal axes of motion and called reconfigurable machine tools (RMTs). These machines may be included in large-scale reconfigurable machining systems (RMSs). When the axes of the machine are non-orthogonal, the movement between the axes is tightly coupled and the importance of coordinated movement among the axes becomes even greater. In the case of a non-orthogonal RMT, in addition to the contour error, another machining error called in-depth error is also generated due to the non-orthogonal nature of the machine. The focus of this study is on the conceptual design of a new type of cross-coupling controller for a non-orthogonal machine tool that decreases both the contour and the in-depth machining errors. Various types of cross-coupling controllers, symmetric and non-symmetric, with and without feedforward, are suggested and studied. The stability of the control system is investigated, and simulation is used to compare the different types of controllers. We show that by using cross-coupling controllers the reduction of machining errors are significantly reduced in comparison with the conventional de-coupled controller. Furthermore, it is shown that the non-symmetric cross-coupling feedforward (NS-CC-FF) controller demonstrates the best results and is the leading concept for non-orthogonal machine tools. [DOI: 10.1115/1.1771692]

1 Introduction

Currently manufacturing industries have two primary methods for producing medium and high volume machined parts: dedicated machining systems (DMSs) and flexible manufacturing systems (FMSs) that include CNC machines. The DMS is an ideal solution when the part design is fixed and mass production is required to reduce cost. On the other hand, the FMS is ideal when the required quantities are not so high and many modifications in the part design are foreseen. In contrast to these two extremes, Koren [1,2] describes an innovative approach of customized manufacturing called reconfigurable manufacturing systems (RMS). The main advantage of this new approach is the customized flexibility in the system to produce a ''part family'' with lower investment cost than FMS. A typical RMS includes both conventional CNC machines and a new type of machine called the Reconfigurable Machine Tool [3]. The Engineering Research Center (ERC) for Reconfigurable Machining Systems (RMS) at the University of Michigan with its industrial partners has designed an experimental Reconfigurable Machine Tool (RMT) [4]. This machine allows ERC researchers to validate many of the new concepts and machine tool design methodologies that have been already developed in the center. There are many types of RMTs. This paper describes an arch-type non-orthogonal multi-axis RMT machine as shown in Figure 1, and Figure 2. The economic justification of RMTs is given in section 2 of this paper.

A contouring motion requires that the cutting tool moves along a desired trajectory. Typically, computerized control systems for machine tools generate coordinated movements of the separately driven axes of motion in order to trace a predetermined path of the

cutting tool relative to the workpiece [5]. To reduce the contouring error, which is defined as the distance between the predetermined and the actual path, there have been two main control strategies. The first approach is to use feedforward control in order to reduce axial tracking errors [6,7] however, they are limited when non-linear cuts are required [8]. The other approach is to use cross-coupling control [8–11] in which axial-feedback information is shared between the moving axes. The cross-coupling controller is used in addition to the conventional axial servo controller. At each sampling time, the cross-coupling controller calculates the current contour error and generates a command that moves the tool toward the closest point on the desired tool path. This control strategy of the cross-coupling controller (CCC) effectively decreases the contour error.

Advanced control methods have been applied to further improve the control properties of the original cross-coupling controller (CCC). An optimal CCC is suggested in [11], to improve the controller performance when high contouring speeds were required. Another method to overcome the same problem for higher contour feedrates is addressed in [12], which uses adaptive feedrate control strategy to improve the controller performance. The latest trend of cross-coupling controller improvement is the application of fuzzy logic as in [13,14]. All these methods, however, do not work for machines with non-orthogonal axes.

Surface cut (e.g., a circular cut in the *X-Y* plane) on a 3-axis orthogonal milling machine requires a motion of two axes (e.g., *X* and *Y*). However, surface cuts in the non-orthogonal RMT (see Figure 1) require simultaneous motion of all three axes. Therefore, in addition to the contour error, this motion creates another error, called the in-depth error, which is in the *Z* direction. This error affects the surface finish quality of the workpiece. While contouring, the tool tip of the RMT has not only to follow the predetermined path, but also to control continuously the depth of cut. The simultaneous control of both errors, the conventional contour error and the in-depth error, requires a new control strategy since the

standard CCC algorithms cannot be directly applied. In other words, the RMT control design problem requires a new control approach that is able to correct simultaneously two types of cutting errors. This problem has not been addressed in the literature.

In this paper, we describe three types of controllers aimed at reducing the contour and in-depth error simultaneously. First we investigate a symmetrical cross-coupling (S-CC) controller, which unfortunately does not show good performance in reducing both errors. The poor performance is due to the conflicting demands in reducing the two errors and the lack of information sharing between the two pairs of axes (X-Y and Y-Z), which are responsible for error compensation. To overcome this problem, the required motion information of one pair of axes is fed forward to the other. This idea results in two new controller types, symmetrical cross-coupling feedforward (S-CC-FF) controller and non-symmetrical cross-coupling feedforward (NS-CC-FF) controller. Finally, the influence of the reconfigurable angular position of the cutting tool on system stability is investigated.

2 Machine Characteristics and the Control Problem

In this section we explain the economic advantage of the RMT, and develop the mathematical representation of the contour error and the in-depth error.

a Machine Characteristics. Typical CNC machine tools are built as general-purpose machines. The part to be machined has to be adapted to a given machine by utilizing process planning methodologies. This design process may create a capital waste: Since the CNC machine is designed at the outset to machine any part (within a given envelope), it must be built with general flexibility, but not all this flexibility is utilized for machining a specific part. The concept of RMTs reverses this design order: The machine is designed around a known part family. This design process creates a less complex, although less flexible machine, but a machine that contains all the functionality and flexibility needed to produce a certain part family. The RMT may contain, for example, a smaller number of axes, which reduces cost and enhances the machine reliability. Therefore, in principle, a RMT with customized flexibility would be less expensive than a comparable CNC that has general flexibility.

A conceptual example of a RMT designed to machine a part with inclined surfaces of 45 deg is shown in Fig. 1. If a conventional CNC is used to machine this inclined surface, a 4- or 5-axis machine is needed. In this example, however, only three axes are needed on a new type of 3-axis non-orthogonal machine tool. Nevertheless, one may argue that it's not economical to build as product non-orthogonal machine tools for 45 deg. Therefore, we developed a 3-axis non-orthogonal machine in which the angle of the Z-axis is adjustable during reconfiguration periods, as shown in Fig. 2. The simple adjusting mechanism is not servo-controlled and does not have the requirements of a regular moving axis of motion.

The designed RMT may be reconfigured into six angular positions of the spindle axis, between -15 and 60 deg with steps of 15 deg. The main axes of the machine are X-axis (table drive horizontal motion), Y-axis (column drive vertical motion) and Z-axis (spindle drive inclined motion) as in Fig. 1. The two extreme positions of the machine spindle axis (-15 and 60 deg) are shown in Fig. 3. The XYZ machine axes comprise a non-orthogonal system of coordinates, except for the case when the spindle is in a horizontal position. Two orthogonal auxiliary systems of coordinates are used to describe the machine, XSZ and XYZ', where S is an axis parallel to the part surface and Z' is an axis perpendicular to both X and Y-axis.

The machine is designed to drill and mill on an inclined surface in such a way that the tool is perpendicular to the surface. In milling at least two axes of motion participate in the cut. For example, the upward motion on the inclined surface in the S-axis direction requires that the machine drive move in the positive Y
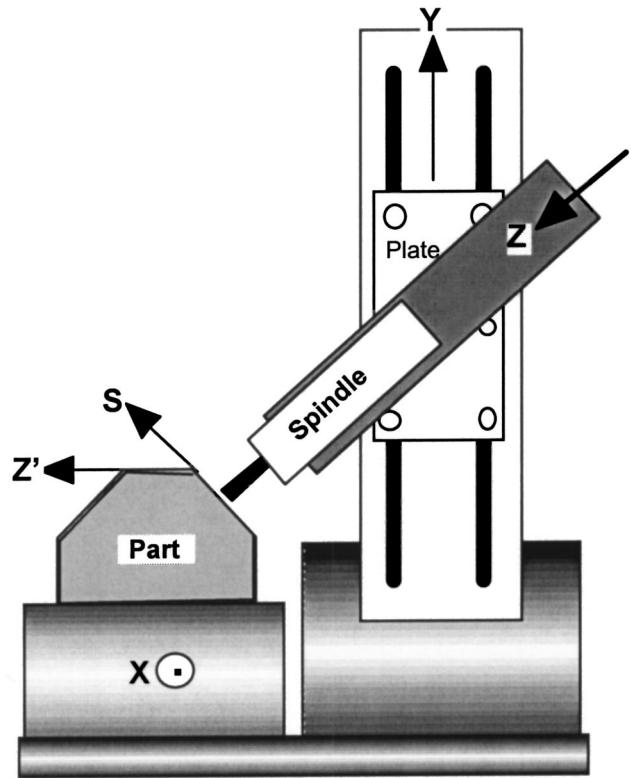

Fig. 1 Schematic view of a Reconfigurable Machine Tool

direction (upward) and in the positive Z direction (downward). When milling a nonlinear contour (e.g., a circle) on the inclined surface of the RMT, we may expect to get the traditional contour error. This error is measured on the workpiece surface (X-S plane) relative to the predetermined required path of the tool. However, in our machine, we get additional cutting error at the same time. This error is created due to the fluctuations in the depth of cut as result of the combined motion in the Y and Z-axis and therefore we call it "in-depth error." This combined motion is required in order to move the tool up and down along the inclined surface. Figure 4 describes three systems of coordinates. XYZ is the machine tool non-orthogonal system of coordinates where the table
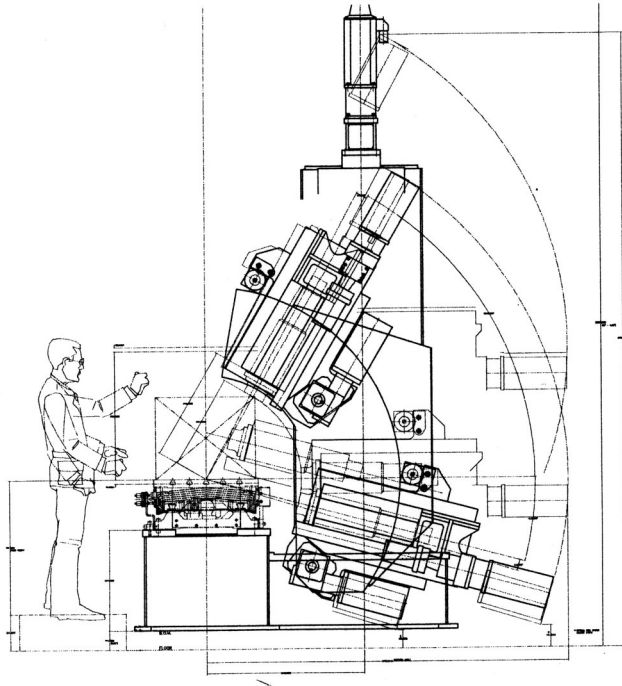

Fig. 2 Arch Type RMT

Fig. 3 Reconfigurable position of Z-axis. The inclined angle can be changed from −15 deg to 60 deg

moves in X direction, Y is the motion along the column and Z is in the direction of the spindle and the cutting tool. XSZ is an auxiliary orthogonal system of coordinates where S is the direction of the inclined surface of the workpiece, which is perpendicular to the tool axis. XYZ' is another auxiliary orthogonal system of coordinates where Z' is horizontal.

b   Contouring and In-Depth Errors.   To overcome the combined error, we designed a special cross-coupling controller. In the present paper, we would like to explain some aspects of the controller design. This design of a new cross-coupling controller for the 3-axes of motion gives insight to the system behavior under external disturbances.

Contouring Error: The contouring error is described in many papers [e.g., [8–14]]. A general non-linear curve approximated by an instantaneous circle on which a contour error is defined as given by Lo [15]. Figure 5a shows the contour and the "in depth" errors. Figure 5b shows the contour error of a curved contour. The contour error equation in the RMT machine is
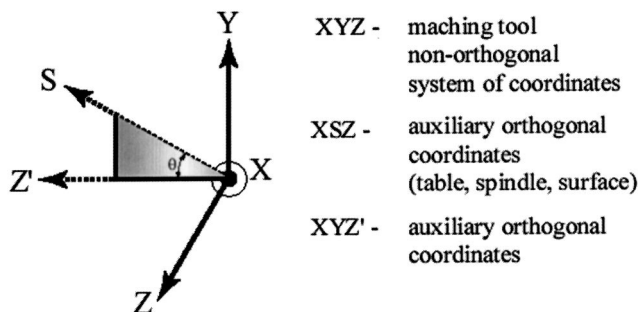
System of Coordinates

XYZ -	maching tool non-orthogonal system of coordinates
XSZ -	auxiliary orthogonal coordinates (table, spindle, surface)
XYZ' -	auxiliary orthogonal coordinates

Fig. 4   Systems of coordinates

$$\varepsilon_r = -C_{rx}\cdot E_x + C_{ry}\cdot E_y$$

$$\text{Where,}\quad C_{rx} = \sin(\phi) - \frac{E_x}{\rho^2}$$

$$C_{ry} = \frac{\left(\cos(\phi) - \dfrac{E_y}{\rho^2}\right)}{\sin(\theta)} \tag{1}$$

Since θ varies between 30° and 105°, the singularity of C_{ry} does not need to be considered.

In-depth Error: The in-depth error is typical to the characteristics of our non-orthogonal machine. In order to cut the workpiece at a predetermined depth, the combined motion of both Y and Z-axis must be controlled. As a result of the position errors of the servomotor drives due to the external disturbances on each axis the in-depth error is generated. This error may affect significantly the quality of the surface finish. The in-depth error is described in Figure 5c. Equation (2) describes the linear relation between the error components in the Y and Z directions. It is important to understand that this error is not only time dependent but also depends on the machine reconfiguration angular position. For each angle of spindle axis positioning, the controller will apply different value of C_{zy} in equation (2).

$$\varepsilon_z = -C_{zy}\cdot E_y + C_{zz}\cdot E_z$$

where

$$C_{zy} = \cos(\theta)$$

$$C_{zz} = 1 \tag{2}$$

It is important to notice that the position error of Y-axis E_y appears on both Eqs. (1) and (2). This implies tight coupling between the contour error and the in-depth error. The RMT controller should decrease both errors effectively.

3   Controllers Design

In traditional orthogonal CNC machines, the cross-coupling control strategy effectively reduces the error between the predetermined tool path and the actual tool path. In a two-axis contouring system, the X-axis servodrive receives two inputs: one a traditional input from an X-axis servo controller that reduces E_x (the axial position error along the X direction) and another input from the cross-coupling controller to reduce ε_{rx} (the X component of the contour error). Similarly, the Y-axis plant receives two inputs. The additional inputs to each axis are used to decrease the contour error in the normal direction represented by ε_r in Fig. 5b.

The objective of this paper is to suggest a suitable cross-coupling control strategy for both the contour and in-depth errors. Three controllers are examined: a symmetric cross-coupling (S-CC) controller, the symmetric cross-coupling controller with additional feedforward (S-CC-FF), and a non-symmetric cross-coupling controller with feedforward (NS-CC-FF).

a   Controllers Structures.   The detailed structure of the three controllers is illustrated in Fig. 6. The basic structure is to have two standard cross-coupling (CC) controllers, one for the contour error in the XY-subsystem with a gain G_r and the other for the in-depth error in the YZ-subsystem with a gain G_z. Section 4b includes a discussion on the values of G_r and G_z. The in-depth cross-coupling controller has the same basic control structure as the contour cross-coupling controller. In addition, a feedforward term may be used to inform the Z-axis about the additional Y-axis input caused by the contour cross-coupling controller. "Knowing" this information in advance, the Z-axis can compensate for the movement of the Y-axis in order to reduce the in-depth error.

The differences among the three proposed controllers are: (a) the presence or absence of a feedforward term (In the S-CC controller, the K_{ff} block does not exist), and (b) a difference in the
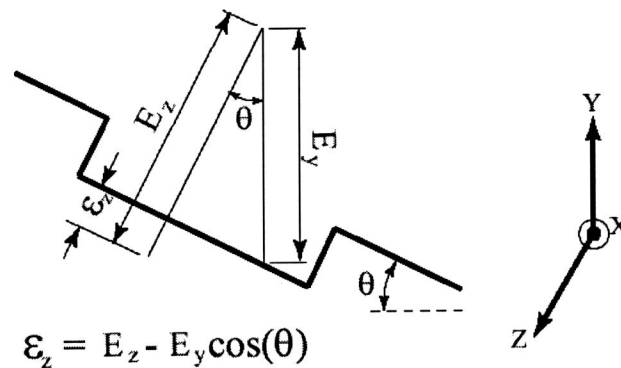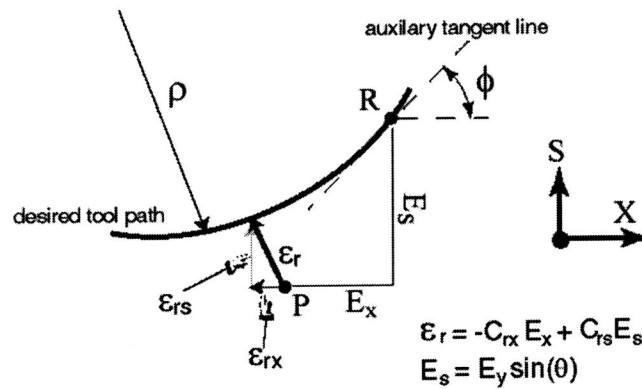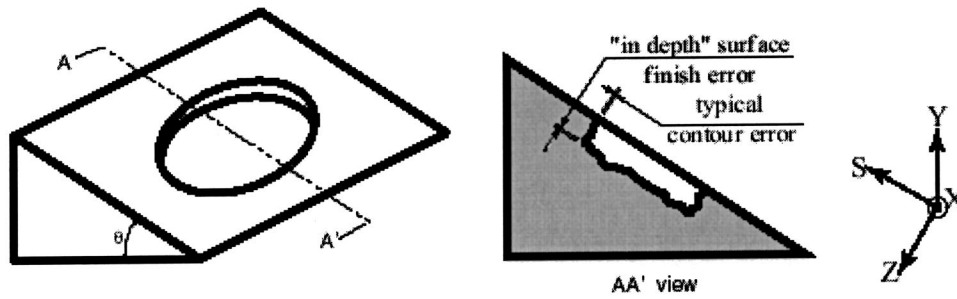
$$\varepsilon_r = -C_{rx} E_x + C_{rs} E_s$$
$$E_s = E_y \sin(\theta)$$

$$\varepsilon_z = E_z - E_y \cos(\theta)$$

Fig. 5 Comparison between axial error and tracing error

direction of the controlling error (in the NS-CC-FF controller, C_{zy} is zero). If the feedforward term exists, K_{ff} in Figure 6 can be expressed as follows

$$K_{ff} = \cos(\theta) \cdot \frac{\mathrm{DCgain}(H_z)}{\mathrm{DCgain}(H_y)} \qquad (3)$$

The tracing error estimation gains, C_{rx}, C_{ry}, C_{zy}, C_{zz} are given in Equations (1) and (2).
The symmetric cross-coupling (S-CC) controller uses the contour cross-coupling controller between the X and Y-axis and the in-

depth cross-coupling controller between the Y and Z-axis. The contour cross-coupling controller decreases the contour error by coupling the X and Y-axis movements while the in-depth cross-coupling controller compensates the in-depth error by coupling the Y and Z-axis movements. The Y-axis receives one output from each cross-coupling controller; U_{ry} and U_{zy}. As briefly explained in the previous section, U_{ry} and U_{zy} may be in conflict with each other and the resulting control action does not necessarily decrease both the contour and the in-depth error. This is the main drawback of the SCC controller and it will be further investigated in the stability section.
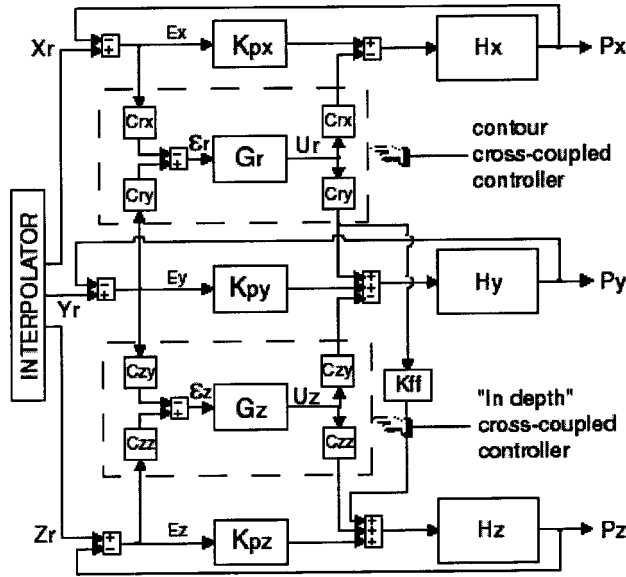
Fig. 6 The diagram of the Symmetric Cross-Coupled Feed-Forward (S-CC-FF) controller. In the S-CC controller, the feed-forward block, K_{ff}, does not exist. In the Non-Symmetric controller (NS-CC-FF), C_{zy} is zero.

The symmetric cross-coupling feedforward (S-CC-FF) controller has the same structure as the S-CC controller, but includes an additional feedforward term. This feedforward term gives the Z-axis information about the movement of the Y-axis. In other words, when an output from the contour cross-coupling controller is applied to the Y-axis, this additional input is fed to the Z-axis in order to reduce the in-depth error from that additional input to Y-axis. Even though the S-CC-FF controller improves the performance of the system by adding a feedforward term, the conflict between the cross-coupling controllers still exists. Again, this characteristic will be discussed in more detail in the stability section. This is the motivation for introducing the next controller.

The non-symmetric cross-coupling feedforward (NS-CC-FF) controller is suggested in order to remove the coupling between the cross-coupling controllers. Even though the in-depth error depends on the performance of the Y and Z-axis, this error is always parallel to the Z-axis movement. Using this characteristic we convert the controller to a master (Y)-slave (Z) operation in which the controller moves only the Z-axis to decrease the in-depth error. Namely, the coupling between the contour cross-coupling controller and the in-depth cross-coupling controller is removed in the NS-CC-FF controller. Therefore, Y-axis servo drive receives only one output from the cross-coupling controllers. As will be shown later this controller has the best performance.

4 Controllers Stability Analysis

The RMT system has tightly coupled axes and contains time-varying sinusoidal parameters. In order to simplify the stability analysis, the following assumption was made: $\varepsilon \ll E \ll \rho$, where ε, E, ρ are contour error, axial error, and radius of curvature, respectively [15]. With this assumption, for the stability analysis, we can approximate the sinusoidal gains by linear terms. Furthermore, in order to eliminate the complexity with time-varying parameters in the stability analysis, we analyze the linearized contouring system since the cross-controller gains, C_{rx}, C_{ry}, C_{zy} and C_{zz} are constants in this case. The analysis below shows that there are bounded stability regions, and the controller parameters must be selected to satisfy certain constraints in order for the system to be stable.

a. Characteristic Equations of S-CC, S-CC-FF, and NS-CC-FF Controllers. For the linear system, $\dot{X} = A \cdot X + B \cdot U$, $Y = C \cdot X + D \cdot U$, the transfer function from U to Y, which is $C(sI\text{-}A)^{-1}B + D$, should be examined for the stability of the system. However, if C and D are BIBO matrix, then $(sI\text{-}A)^{-1}B$ can be used for the stability analysis. Since the C and D matrices for the contour and in-depth error of the RMT are bounded time varying gain matrices, the stability of each axis can be used for the stability analysis of the entire system. For S-CC controller the positions of each axis are given as follows

$$P_x = \frac{(C_{rx}^2 \cdot G_r + K_{px}) \cdot H_x}{X_1} X_r - \frac{C_{rx} \cdot C_{ry} \cdot G_r \cdot H_x}{X_1} E_y$$

$$P_y = \frac{(C_{ry}^2 \cdot G_r + C_{zy}^2 \cdot G_z + K_{py}) \cdot H_y}{Y_1} Y_r - \frac{C_{rx} \cdot C_{ry} \cdot G_r \cdot H_y}{Y_1} E_x$$

$$- \frac{C_{zy} \cdot C_{zz} \cdot G_z \cdot H_y}{Y_1} E_z$$

$$P_z = \frac{(C_{zz}^2 \cdot G_z + K_{pz}) \cdot H_z}{Z_1} Z_r - \frac{C_{zy} \cdot C_{zz} \cdot G_z \cdot H_z}{Z_1} E_y \quad (4)$$

where

$$X_1 = 1 + (C_{rx}^2 \cdot G_r + K_{px}) \cdot H_x$$

$$Y_1 = 1 + (C_{ry}^2 \cdot G_r + C_{zy}^2 \cdot G_z + K_{py}) \cdot H_y$$

$$Z_1 = 1 + (C_{zz}^2 \cdot G_z + K_{pz}) \cdot H_z$$

The notations P_x, P_y, P_z indicate the positions of the X, Y, Z-axis, respectively. X_r, Y_r, Z_r are the reference signals for each axis, and E_x, E_y, E_z are the errors ($E_x = X_r - P_x$). For the S-CC-FF controller the positions are

$$P_x = \frac{(C_{rx}^2 \cdot G_r + K_{px}) \cdot H_x}{X_2} X_r - \frac{C_{rx} \cdot C_{ry} \cdot G_r \cdot H_x}{X_2} E_y$$

$$P_y = \frac{(C_{ry}^2 \cdot G_r + C_{zy}^2 \cdot G_z + K_{py}) \cdot H_y}{Y_2} Y_r - \frac{C_{rx} \cdot C_{ry} \cdot G_r \cdot H_y}{Y_2} E_x$$

$$- \frac{C_{zy} \cdot C_{zz} \cdot G_z \cdot H_y}{Y_2} E_z$$

$$P_z = \frac{(C_{zz}^2 \cdot G_z + K_{pz}) \cdot H_z}{Z_2} Z_r - \frac{C_{rx} \cdot C_{ry} \cdot G_r \cdot K_{ff} \cdot H_z}{Z_2} E_x$$

$$- \frac{(C_{zy} \cdot C_{zz} \cdot G_x + C_{ry}^2 \cdot G_r \cdot K_{ff}) \cdot H_z}{Z_2} E_y \quad (5)$$

where

$$X_2 = 1 + (C_{rx}^2 \cdot G_r + K_{px}) \cdot H_x$$

$$Y_2 = 1 + (C_{ry}^2 \cdot G_r + C_{zy}^2 \cdot G_z + K_{py}) \cdot H_y$$

$$Z_2 = 1 + (C_{zz}^2 \cdot G_z + K_{pz}) \cdot H_z$$

Note that in equations (4) and (5), P_y contains a term that depends on E_z as a disturbance. For the NS-CC-FF controller the axial positions are

$$P_x = \frac{(C_{rx}^2 \cdot G_r + K_{px}) \cdot H_x}{X_3} X_r - \frac{C_{rx} \cdot C_{ry} \cdot G_r \cdot H_x}{X_3} E_y$$

$$P_y = \frac{(C_{ry}^2 \cdot G_r + K_{py}) \cdot H_y}{Y_3} Y_r - \frac{C_{rx} \cdot C_{ry} \cdot G_r \cdot H_y}{Y_3} E_x$$

$$P_z = \frac{(C_{zz}^2 \cdot G_z + K_{pz}) \cdot H_z}{Z_3} Z_r - \frac{C_{rx} \cdot C_{ry} \cdot G_r \cdot K_{ff} \cdot H_z}{Z_3} E_x$$

$$- \frac{C_{ry}^2 \cdot G_r \cdot K_{ff} \cdot H_z}{Z_3} E_y \qquad (6)$$

where

$$X_3 = 1 + (C_{rx}^2 \cdot G_r + K_{px}) \cdot H_x$$

$$Y_3 = 1 + (C_{ry}^2 \cdot G_r + K_{py}) \cdot H_y$$

$$Z_3 = 1 + (C_{zz}^2 \cdot G_z + K_{pz}) \cdot H_z$$

The following is a summary of observations related to the characteristic equations of the three proposed controllers.

$$X_1 = X_2 = X_3$$

$$Y_1 = Y_2$$

$$Z_1 = Z_2 = Z_3$$

Namely, the characteristic equation of the X-axis, is the same in all three controllers. However, the characteristic equations of the Y and Z-axis depend on the type of controller used. In order to simplify the analysis the stability analysis is done for a given stable servo controllers for each axis and we investigate the stability of the system due to the cross-coupling controllers, G_r and G_z, only.
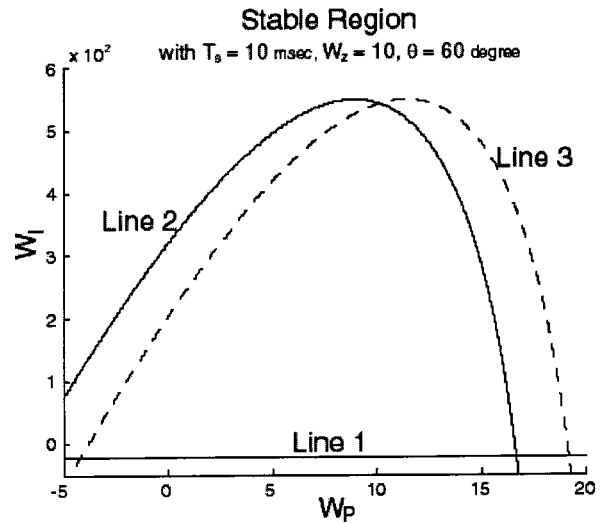
b   Stable Region of the Cross-Coupling Controllers.   The characteristic equations obtained in the previous section depend not only on the variable gain, C's, but also on the RMT configuration angle, θ. Furthermore, the characteristic equation for Y with the S-CC and S-CC-FF controllers exhibit coupling between the contour and in-depth cross-coupling controllers. In order to simplify the analysis, **PI** controller for G_r and **P** controller for G_z are used

$$G_r = W_P + \frac{W_I \cdot T_s}{z - 1}$$

$$G_z = W_z \quad \text{where } W_P, \ W_I, \text{ and } W_z \text{ are gains} \qquad (7)$$

Numeric values of the parameters used in this study to describe the servo controllers and the plants are presented in appendix A. Utilizing these values, the characteristic equation can be expressed in terms of W_P, W_I, W_Z, C's, and θ. First, the configuration of the RMT system is fixed at $\theta = 60°$, and the characteristic equation is calculated as function of W_P, W_I, W_Z, and C's. Using the Routh-Jury criteria, the stable regions of W_P, W_I, and W_Z are obtained as a function of C's, and the smallest intersection of the stable regions with respect to C's values was obtained. In addition, two sampling periods were considered, $T_s = 10$ msec and $T_s = 1$ msec. One typical stability plot for $W_z = 10$ and $\theta = 60°$, is shown in Fig. 7. The stability analysis results may be summarized as follows:

1. The stable region for S-CC and S-CC-FF controllers is an area bounded by three lines (as shown in Fig. 7): Line 1, Line 2, and Line 3 while the stable region for NS-CC-FF controller is the area bounded by Line 1 and Line 3.
2. For higher values of the gain W_z, Line 2 moved to the left while Line 1 and Line 3 were not affected by varying W_z. It means that a higher value of the proportional controller gain W_z, will reduce the stability region.

a. $T_s = 10$ *msec*
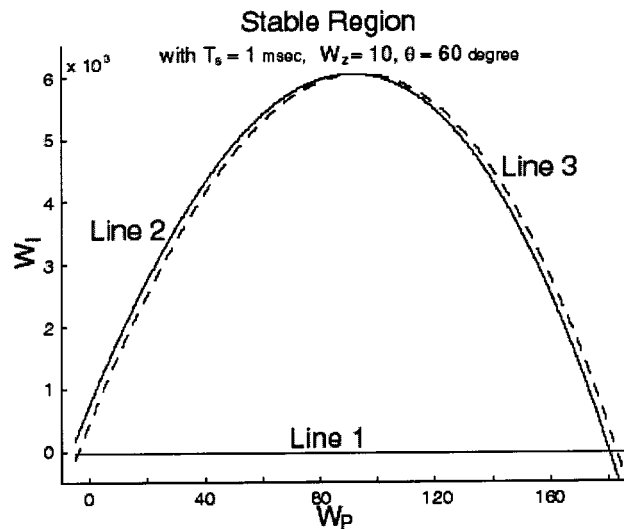
b. $T_s = 1$ *msec*

Fig. 7   Stable region for the parameters of the cross-coupled controllers

3. For higher θ values, Line 2 moves to the right while Line 1 and Line 3 are not affected. However, Line 2 can never cross Line 3 by only varying θ. The meaning of this observation is that horizontal spindle position represents better stability of the system.
4. The stability region becomes smaller with increasing sampling period.

The system with the NS-CC-FF controller has the largest stable region for W_P, W_I, and W_Z. This is due to the fact that the conflict between the cross-coupling controllers has been removed by decreasing the in-depth error by Z-axis movement only. The conflict between the cross-coupling controller in S-CC and S-CC-FF controller can be seen in the transfer function shown in Eqs. (4) and (5). The subsystem for the contour error, which consists of X and Y-axis only, should contain only variables related to the X and Y-axis such as E_x, E_y, X_r, and Y_r. However, this subsystem contains also an E_z term. This E_z term will act as a disturbance to the contour subsystem.
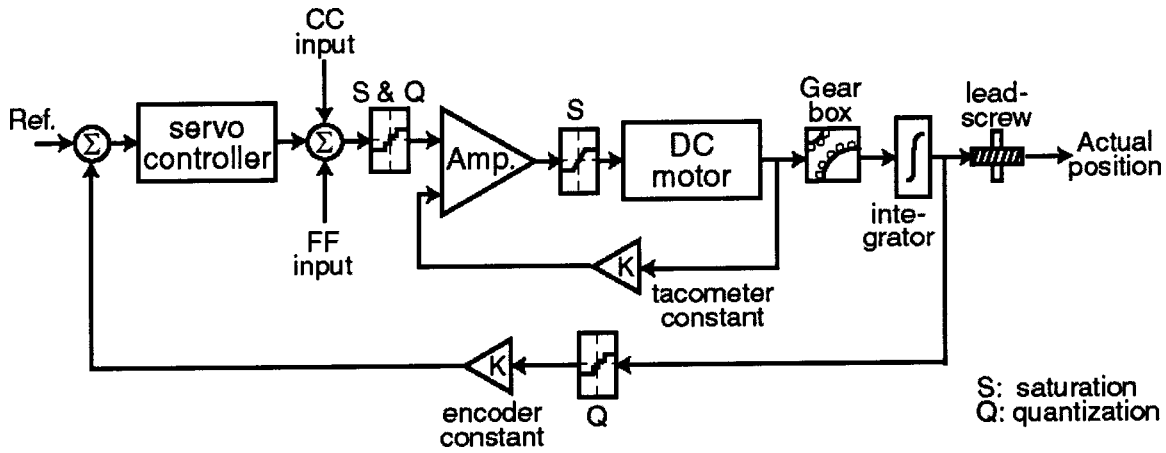
Fig. 8   The simplified RMT axial model

Similarly, the subsystem for the in-depth error, which consists of Y and Z-axis only, should be composed of terms related to the Y and Z-axis. Again, the in-depth subsystem contains an E_x term which will act as a disturbance to this subsystem. Unlike the transfer function of the Z-axis in Eq. (4), the one in Eq. (5) contains a feedforward term K_{ff}. This K_{ff} reduces the disturbance to the system resulting in a better performance for the S-CC-FF than the S-CC controller. Considering the transfer functions for the NS-CC-FF controller shown in Eq. (6), the subsystem for the contour error contains only terms related to the X and Y-axis and the subsystem for the in-depth error contains a feedforward term K_{ff} that compensates the disturbance term. In other words, the disturbance term from the contour cross-coupling controller to the in-depth cross-coupling controller was removed using the feedforward term. Also the disturbance term from the in-depth cross-coupling controller to the contour cross-coupling controller was removed by correcting the in-depth error by only moving the Z-axis. Overall, the performance of the system using NS-CC-FF controller is expected to be the best among the proposed controllers, and the simulation results support this analysis.

5   Simulation Results

The simplified RMT axial model that was used in the simulation is shown in Fig. 8 (the parameters for each axis can be found in appendix A). The cross-coupling controller parameters were chosen such that the system will operate within the stable region defined in the previous section. These parameters are not the optimal since optimization of the controller, was not a goal of this paper. For comparison purposes, all cross-coupling controller parameters are kept the same throughout the simulation. The desired tool path is a circular motion on the inclined X-S plane, and the response of each controller to a disturbance is compared.

Figures 9, 10 and 11 describe simulation results. Figure 9-a shows results of a contour error in a circular cut on the S-plane. Without disturbances all three proposed CC controllers (that converge into one line on the figure) give better results than the decoupled control. Figure 9-b shows the results of in-depth error control without disturbances. In this case it is clear that the symmetrical CC controller (S-CC) has poor performance. Figure 10-a and 10-b show simulation results with a step disturbance in the Y-axis direction (along the column of the machine). The trends of the results are similar to those of Fig. 9. In the presence of disturbance acting on the Y-axis, the performance difference between S-CC-FF and NS-CC-FF controllers is insignificant as shown in Fig. 10. Figure 11-a and 11-b show simulation results due to a step disturbance in the Z-axis direction (along the spindle axis). Figure 11-a shows that for a contour error all three CC controllers operate better than the decoupled control, but the NS-CC-FF controller presents the best performance. The contour error of the

NS-CC-FF controller is not affected by the disturbance in Z-axis, while the contour error plot of S-CC-FF has an abrupt jump. Similarly, for the in-depth error, the NS-CC-FF controller shows better performance than the S-CC controller as may be seen in Fig. 11-b. To summarize the results, we may conclude that all simulation results shows that the performance of the NS-CC-FF controller is superior in all circumstances, as was expected at the design stage.

6   Conclusions

The conceptual design process of crossed-coupling controllers that was described in the paper allows insight and better understanding of the RMT controller problem. Some machining processes that traditionally require four or 5 degrees-of-freedom us-
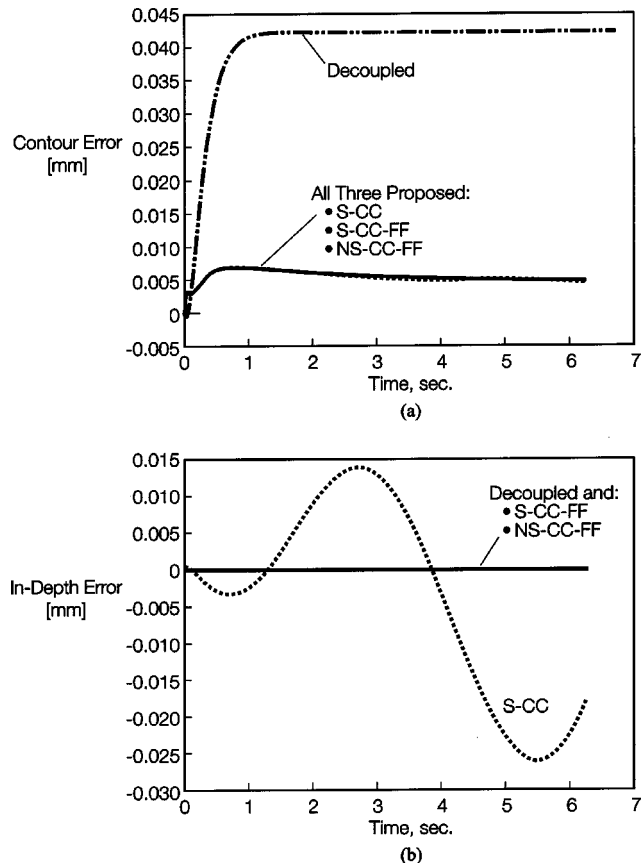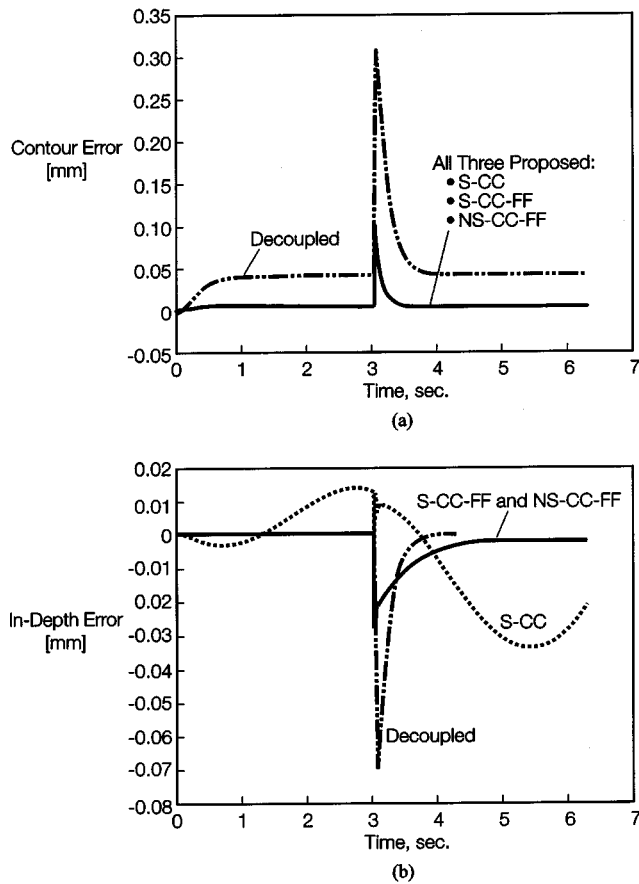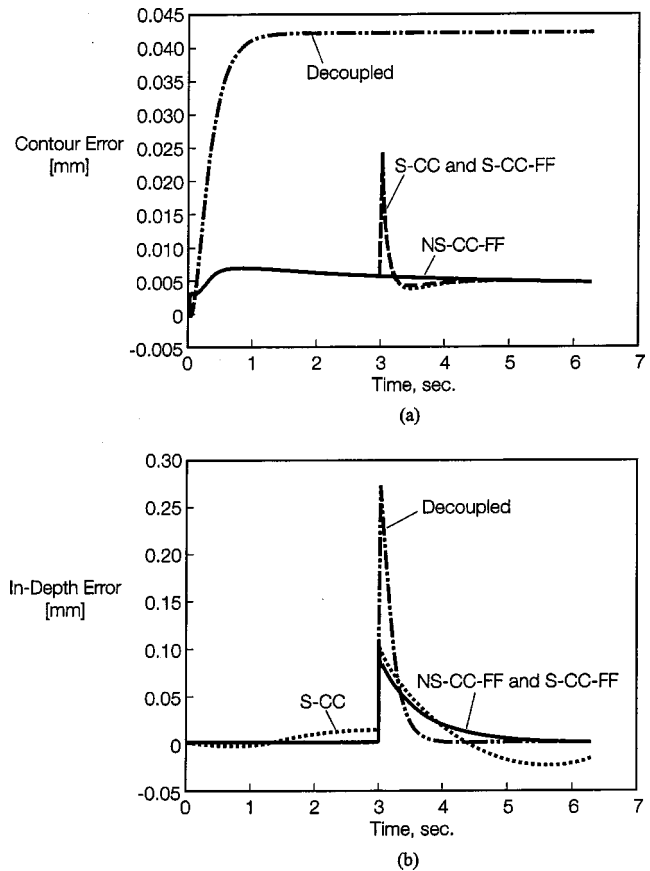

Fig. 9   Simulation results without any disturbance

Fig. 10 Simulation results with a step disturbance in the *Y*-**axis**

Fig. 11 Simulation results with a step disturbance in the *Z*-**axis**

ing an orthogonal CNC machine, may be performed by a new machine-type—the reconfigurable machine tool (RMT) that has just three-degrees of freedom. The disadvantage of the RMT configuration is that when contour cuts are needed in the *X-S* plane, a new type of error—the in-depth error—may occur. This error, if not controlled properly, may severely affect the surface finish of the machined surfaces. To reduce the effect of the in-depth error, we introduced three types of cross-coupling controllers and found that all three are stable for a reasonable range of parameters. An increase of the reconfiguration angle (or tool-positioning angle) increases the contour and in-depth errors and decreases the region of stability.

Furthermore, we also found that all three types of cross-coupling (CC) controllers reduce significantly the contour and in-depth errors. It was shown that for the control of the nonorthogonal arch-type RMT, the nonsymmetric cross-coupling feed-forward (NS-CC-FF) controller has the best performance of the

three CC controllers. The symmetric cross-coupling (S-CC) controller does not adequately solve the in-depth error problem-an error that is typical to non-orthogonal RMTs. The S-CC-FF controller is marginally acceptable, but has problems when a disturbance (such as a cutting force) is applied to the Z-axis. Only the NS-CC-FF controller reduces significantly both the contour and the in-depth errors. Furthermore, the stability analysis shows that the NS-CC-FF controller is stable for a wider range of parameters than the other controllers are. Our main conclusion is, therefore, that the NS-CC-FF controller best fits the arch-type RMT. Nevertheless, we cannot state that it is a general conclusion for all types of RMTs.

Acknowledgment

Appendix—Simulation Parameters

X-axis data	
NX = 1/10;	gear box ratio
MX = 1000;	mass of table [Kg]
LX = 10;	lead of the screw [mm/rev]
JlX = 0.0008;	lead screw inertia [Kg-m²]
K_ampX = 20;	amplifier gain
Amp_max X = 200;	amplifier maximum voltage
Amp_min X = −200;	amplifier minimum voltage
K_tachX = 0.001;	tachometer gain [volts/(rad/sec)]
K_encoderX = 1000;	encoder gain [pulses/rev]
K_pulse2mmX = LX/K_encoderX;	encoder pulses to position conversion
DAC_max X = 10;	DAC maximum voltage
DAC_min X = −10;	DAC minimum voltage

DAC_bitX=16;	number of bits used to convert digital signal to analog voltage
KtX=0.1;	motor torque constant [N-m/A]
KvX=0.1;	voltage constant (=back-emf constant) [V/(rad/sec)]
JmX=0.0004;	motor rotor inertia [Kg-m^2]
LaX=0;	armature inductance [Henry] negligible;
RaX=0.5;	armature resistance [Ohm]
BmX=0;	viscous-friction coefficient [N-m/(rad/sec)] negligible;
PGainX=4.2;	servo controller P gain
IGainX=21;	servo controller I gain
DGainX=0;	servo controller D gain

Y-axis data=X-axis data
Z-axis data=X-axis data

References

[1] Koren, Y., 1999, ''Reconfigurable Machining Systems Vision with Examples,'' ERC/RMS Report #19, The University of Michigan, Ann Arbor.

[2] Koren, Y., Jovane, F., Heisel, U., Pritschow, G., Ulsoy, G., and VanBrussel, H., 1999, ''Reconfigurable Manufacturing Systems,'' A Keynote paper. CIRP Ann., **2**, pp. 6–12.

[3] Koren Y. and Kota S. (inventors): Reconfigurable Machine Tool. U.S. patent #5,943,750. Issue date 8/31/1999.

[4] Katz, R., Chung, H., 1999, ''Design of an Experimental Arch Type Reconfigurable Machine Tool,'' ERC/RMS Report #22, The University of Michigan, Ann Arbor.

[5] Koren, Y., 1983, ''Computer Control of Manufacturing Systems,'' McGraw-Hill, New York.

[6] Tomizuka, M., 1987, ''Zero Phase Error Tracking Algorithm for Digital Control,'' ASME J. Dyn. Syst., Meas., Control, **109**, March, pp. 65–68.

[7] Tomizuka, M., 1988, ''Design of Digital Tracking Controllers for Manufacturing Applications,'' *Control Methods for Manufacturing Processes*, DSC-Vol. 9, ASME, New York.

[8] Koren, Y., 1980, ''Cross-coupling Biaxial Computer Control for Manufacturing Systems,'' J. Dyn. Syst., Meas., Control, **102**, December, pp. 265–272.

[9] Koren, Y. Lo Ch.-Ch. 1991, ''Variable-Gain Cross-Coupling Controller for Contouring,'' CIRP Ann., **40/1/1991**, pp. 321–374.

[10] Srinivasan, K., and Kulkarni, P. A., 1990, ''Cross-coupling Control of Biaxial Feed Drive Servomechanisms,'' J. Dyn. Syst., Meas., Control, **112**, June, pp 225–232.

[11] Kulkarni, P. A., and Srinivasan, K., 1989, ''Optimal Contouring Control of Multi-axial Feed Drive Servomechanisms,'' J. Eng. Ind., **111**, May, pp. 140–147.

[12] Chuang, H., and Liu, C., 1991, ''Cross-coupling Adaptive Feedrate Control for Multiaxis Machine Tools,'' J. Dyn. Syst., Meas., Control, **113**, June, pp. 451–457.

[13] Yeh, Z.-M., Trang, Y. S., and Lin, Y. S., 1997, ''Cross-coupling Fuzzy Logic Control for Multiaxis Machine Tools,'' Mechatronics, **7**, No 8, pp. 663–681.

[14] Yeh, Z.-M., 1998, ''A Cross-coupling Bistage Fuzzy Controller for Biaxis Servomechanism Control,'' Fuzzy Sets Syst., **97**, (1998) pp. 265–275.

[15] Lo, C., 1992, ''Cross-Coupling Control of Multi-Axis Manufacturing Systems,'' Ph.D. Thesis, University of Michigan, Ann Arbor, MI.